Hindawi Publishing Corporation
Journal of Chemistry
Volume 2015, Article ID 561350, 7 pages
http://dx.doi.org/10.1155/2015/561350

Research Article

Ru-Sn-B/Al_2O_3 Catalysts for Selective Hydrogenation of Methyl Oleate: Influence of the Ru/Sn Ratio

María A. Sánchez, Vanina A. Mazzieri, María A. Vicerich, Carlos R. Vera, and Carlos L. Pieck

Instituto de Investigaciones en Catálisis y Petroquímica (INCAPE) (FIQ-UNL, CONICET), Colectora Ruta Nacional, No. 168, Km. 0, Paraje El Pozo, 3000 Santa Fe, Argentina

Correspondence should be addressed to Carlos R. Vera; cvera@fiq.unl.edu.ar

Received 9 September 2015; Accepted 11 November 2015

Academic Editor: Antonio M. Romerosa-Nievas

This study focuses on the influence of the Ru/Sn ratio on the catalytic hydrogenation of methyl oleate to oleyl alcohol using Ru-Sn-B catalysts, notably on the catalytic activity and selectivity. Sn addition acts positively over the oleyl selectivity by reducing the rates of C=O and C=C saturation but also decreases the global activity. The catalyst with the highest activity and selectivity towards oleyl alcohol is Ru(1%)-Sn(2%)-B/Al_2O_3. At a low Sn loading (0.5%) the catalyst has high activity for hydrogenation of the carbonyl group and the carbon-carbon double bond. As a consequence stearyl alcohol is produced with high yield. At a high Sn content (4%) the catalyst has lower selectivity to oleyl alcohol due to its low capacity for hydrogenating the carbonyl group. However it has enough activity for hydrogenating the C=C double bonds to produce the saturated methyl ester.

1. Introduction

Fatty alcohols derived from renewable raw materials are widely used in the production of nonionic amphiphilic tensioactive compounds such as fatty alcohol sulfates, ether sulfates, and alkyl ethoxylate surfactants. Fatty alcohols also find widespread use in the cosmetics industry, being used in the formulation of oily liquid soaps, shampoos and hair conditioners, skin emollients, emulsifiers, and densifying creams and lotions. The main source of fatty alcohols is the catalytic hydrogenation of fatty acid methyl esters over Cu-Cr catalysts under severe reaction conditions (250–350°C and 20–35 MPa) [1, 2]. One concern with these catalysts is the use, handling, and disposal of environmentally hazardous Cr compounds [3] prompting the use of Cr-free catalysts. Another issue is that of the energy-intensive conditions of the Cu-Cr process. More active catalysts could permit using milder process conditions. In this sense and in order to reduce costs and achieve greater selectivity to unsaturated alcohols other alternative catalysts based on supported noble metals have been proposed. In general the reported scientific works show that there are two main groups of catalysts capable of selectively hydrogenating the C=O group in the presence of the double bond C=C, CO-Sn catalysts, and Ru-Sn-B catalysts [1, 4–9].

The influence of the Sn/Ru ratio on the catalyst activity and selectivity has been previously studied by Cheah et al. [10] and Pouilloux et al. [11] with different final results. According to Cheah et al. [10], the maximum selectivity to oleyl alcohol is found with a Sn/Ru ratio of 2, while Pouilloux et al. [11] reported better selectivities with a Sn/Ru of 4. The probable reasons of this difference may be linked to the different catalyst preparation methods and metal precursors used by these two research groups. In the case of Pouilloux and coworkers [11] they prepared catalysts with a high content of metal and promoters (Sn 4.1–10 wt%, Ru 1.5–2.9 wt%). This corresponds to values of the Sn/Ru atomic ratio of 1.9–5.71.

The role of the Sn/Ru ratio in Pt-Sn-Ru/Al_2O_3 catalysts for the selective hydrogenation of fatty acid methyl esters to fatty alcohols is studied in this work. Catalysts of fixed 1% Ru content and variable Sn content (0.5 to 4 wt%) are used. The focus is put on the analysis of the influence of the Sn/Ru ratio on the metal properties and on the selectivity for

the hydrogenation of the methyl ester to the corresponding fatty alcohol.

2. Materials and Methods

2.1. Catalysts Preparation. The preparation procedure has been described in detail elsewhere [12]. A high-purity γ-alumina (Cyanamid Ketjen CK 300) was used as support. The metal catalysts were prepared by the incipient wetness method, as detailed by Schoenmaker-Stolk et al. [13]. The alumina was impregnated with a solution of the metal salts in the required concentration to get the required content in the final catalysts. The volume used was equal to the pore volume of the alumina samples. The catalysts were first reduced with an excess of sodium borohydride in solution. Finally they were calcined in hydrogen at 300°C. All catalysts are named according to the composition of the metal function, for example, Ru(1%)-Sn(2%)-B.

2.2. Assessment of the Content of the Active Metals. An Inductively Coupled Plasma-Optical Emission Spectroscope (ICP-OES, Perkin Elmer, Optima 2100 DV) was used to determine the composition of the metal phase. Before the analysis the samples were first digested in an acid solution and diluted.

2.3. Temperature Programmed Reduction. First, samples were dried at 120°C blanketed with Ar for 1 h. After cooling to room temperature, they were heated up to 850°C at 10°C min^{-1} in a H_2:Ar stream. A more detailed description of the technique can be found in the report by Sánchez et al. [12].

2.4. Cyclohexane Dehydrogenation. This is a standard test reaction for assessing the properties of the metal function. The test was performed at 300°C and 1 atm using a feed of cyclohexane (1.61 cm^3 h^{-1}) diluted in hydrogen (80 cm^3 min^{-1}). Prior to the reaction samples were reduced at 500°C in flowing H_2 for 1 h. Cyclohexane was supplied by Merck (spectroscopy grade, 99.9% pure).

2.5. CO Chemisorption. The catalyst samples, already previously reduced, were further reduced *in situ* (pure hydrogen, 500°C, 1 h, 60 cm^3 min^{-1}) before starting the tests. Then they were subjected to thorough desorption by stripping with N_2 gas at 500°C and 60 cm^3 min^{-1} for 1 h. Then pulses of CO were sent to the cell until saturation and the amount of CO was recorded. More details of the technique can be found elsewhere [14].

2.6. X-Ray Photoelectron Spectroscopy (XPS). The XPS analyses were performed on the solids after an *in situ* treatment with a mixture of H_2:Ar at 300°C and after degassing to a residual pressure of 5.9×10^{-7} Pa. For each sample the analyzed regions of the spectrum were those containing the signals due to the Ru $3d_{5/2}$ and Sn $3d_{5/2}$ core levels. The Al 2p line (74.4 eV) was used to calibrate the recorded spectra. Spectrum peak areas were calculated by integration. Peaks were fitted to a 70/30 sum of Gaussian and Lorentzian functions and the background was considered to be of the Shirley type. More technical details can be found in a previous report [14].

2.7. Fourier Transform Infrared Absorption Spectroscopy (FTIR) of Chemisorbed CO. The tests were made using the catalysts pressed into self-supported circular wafers of 2 cm^2 cross section and about 10–20 mg mass. The samples were first reduced *in situ* overnight at 450°C (60 mL min^{-1}, H_2 flow). Then the sample was degassed for 2 h at a vacuum of 10^{-5} bar. The sample was finally brought to room temperature and successive measurements of the IR absorption spectra were recorded after repeatedly dosing CO inside the chamber. The test was continued until saturation of the sample surface with CO was detected. More details of the technique can be found in the report by D'Ippolito et al. [15].

2.8. Methyl Oleate Hydrogenation. Reaction tests were performed at 290°C and 50 atm. The reactor was pressurized with pure hydrogen and 1 g of catalyst was used. The reactant was methyl oleate (Sigma Aldrich, 99%, 4 cm^3) dissolved in *n*-dodecane (Merck, 99%, 60 cm^3). The reactor was a stainless autoclave, stirred at a rate of 800 rpm. Determination and quantification of the reaction products were performed by gas chromatography. The technique and conditions are described elsewhere [14].

In all test, besides the initial methyl oleate and the desired oleyl alcohol, only methyl stearate and stearyl alcohol were detected.

3. Results and Discussion

It must be indicated that one catalyst, Ru(1.0)-Sn(2.0)/Al_2O_3, was previously used in another of our works studying the influence of the support on the catalytic properties [16]. In this sense, for this material the results of TPR, XPS, FTIR-CO, catalytic activity, and selectivity coincide with those already published.

Table 1 shows the ICP-OES results of the catalysts. Differences between theoretical and actual metal contents are minimal. The surface area of the support (180 m^2 g^{-1}) was not altered by the metal addition step because of the small quantities involved (results not shown).

The temperature-programmed reduction (TPR) traces of the bimetallic catalysts are presented in Figure 1. The results for the monometallic Ru and Sn catalysts have been previously presented [12]. Sn displays a broad reduction range spanning from 150 to 550°C, with 2 reduction zones, one at 200–300°C and the other at 380–520°C which suggest the interaction between the support and oxidized Sn species. Reduction of the Sn^{4+} species to metallic Sn° is prevented by the strong interactions of the intermediate Sn^{2+} species with the support, rendering further reduction impossible [17, 18]. Integration of the TPR trace gives the total hydrogen consumption and indicates that in the case of the Sn catalyst an approximate 80% of the original Sn^{4+} is reduced to Sn^{2+} to species.

Table 1: Values of Ru, Sn, and B concentration as determined by ICP-OES.

Catalysts	Ru (wt%)	Sn (wt%)	B (wt%)
Ru(1%)-Sn(0.5%)	1.03	0.47	0.53
Ru(1%)-Sn(1%)	1.11	0.92	0.95
Ru(1%)-Sn(2%)	0.92	1.90	0.38
Ru(1%)-Sn(4%)	1.06	3.53	0.57

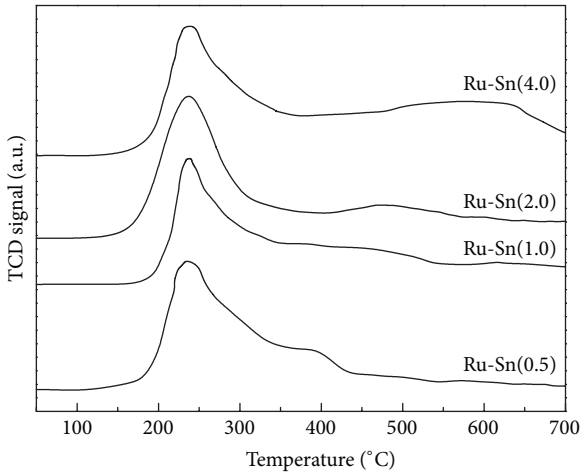

Figure 1: Bimetallic catalysts. Temperature programmed reduction results.

Monometallic Ru catalysts have two TPR reduction peaks at 120°C and 173°C, corresponding to the reduction of chlorinated and oxychlorinated Ru species, respectively [19, 20]. The presence of $RuCl_3$ and other hardly reducible Ru-Cl species in the catalyst is a consequence of an incomplete removal of chlorine during the calcinations steps.

Figure 1 shows that all B-containing Ru-Sn bimetallic catalysts have one reduction peak starting at about 230°C and spanning to 500°C. The peak at lower temperature could be assigned to a simultaneous reduction of Ru and Sn while the tail from 200 to 500°C would be attributed to Sn species segregated from Ru.

The reaction rate of dehydrogenation of cyclohexane (CH) to benzene is proportional to the number of active surface metal atoms; that is, it is indifferent to the structure of the catalyst [21]. In the conditions used, there is no deactivation and the selectivity to benzene is 100%. CO chemisorption is also a useful tool to determine the concentration and properties of the superficial metal atoms. Figure 2 shows the results of cyclohexane conversion and CO/Ru (%) as a function of the Sn content of all the studied catalysts. Additional runs with the monometallic Sn catalyst showed no activity in cyclohexane dehydrogenation and CO chemisorption. It can be seen that both cyclohexane dehydrogenation and CO chemisorption decrease with the content of Sn. The lower dehydrogenating activity of the Ru-Sn catalyst could be ascribed to an electronic or geometric effect of Sn. Both effects have been shown to be present in selective hydrogenation over Pt or Pd modified by chlorine

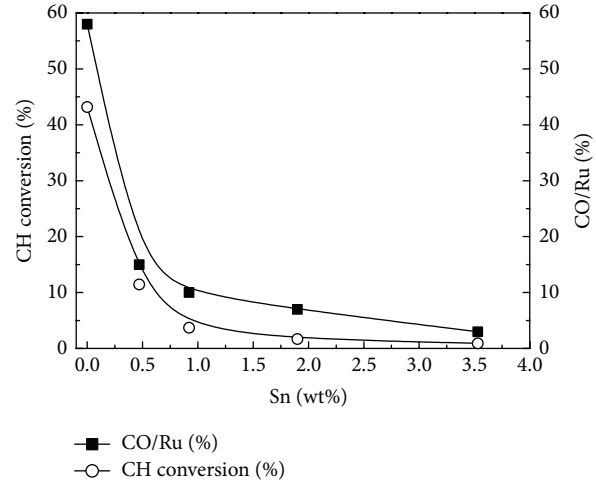

Figure 2: Influence of the Sn content of the catalysts on the conversion of cyclohexane and the CO chemisorption capacity.

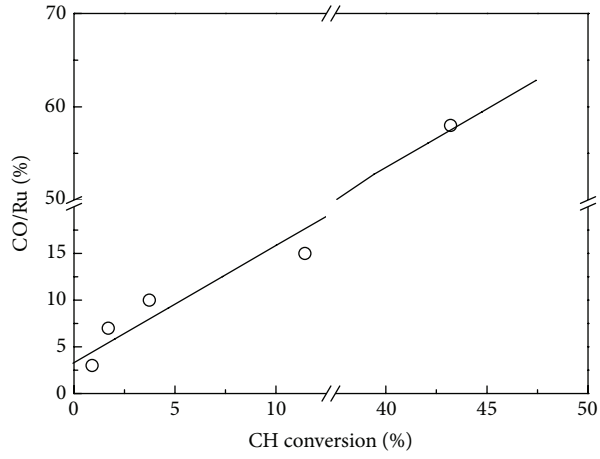

Figure 3: Linear relation between the CO/Ru ratio and the conversion of cyclohexane.

species [22]. However, it has been suggested that for Sn-doped noble metal catalysts the most important effect is the electronic one [23].

Figure 3 shows that the CO/Ru chemisorption capacity increases linearly with cyclohexane dehydrogenation activity, as expected. However the experimental points are slightly deviated from the theoretical line. The difference with respect to the theoretical linear values could be attributed to two different effects. Firstly, an electronic transfer from Sn to Ru would lead to the creation of $Ru^{\delta-}$ species, reducing its adsorption capacity, principally towards H_2 given the lower Ru-H bond strength compared to Ru-CO and Ru-cyclohexane. Secondly, geometrical effects could play a non-negligible role since cyclohexane dehydrogenation requires two contiguous Ru atoms, contrary to CO adsorption [24–26].

The metal interaction was also studied by FTIR analysis of adsorbed CO. As pointed out above, CO is adsorbed over Ru metal sites but it is not adsorbed over Ru metal sites.

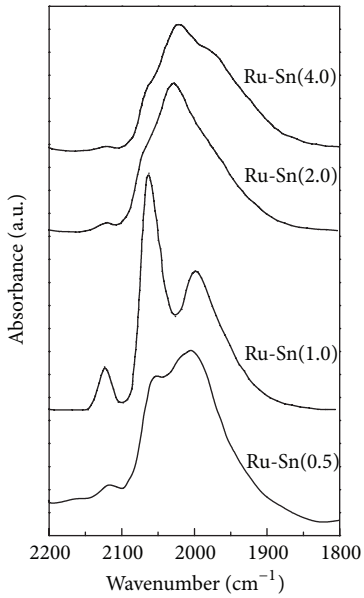

Figure 4: FT-IR spectra of CO adsorbed over the bimetallic catalysts.

The FTIR spectra of chemisorbed CO in the 1800–2200 cm^{-1} wavenumber range are shown in Figure 4. Monometallic Ru catalysts have three characteristic bands, two peaks at 2042 cm^{-1} and 2132 cm^{-1} and a shoulder at about 2080 cm^{-1} [12]. The latter two were assigned to the presence of chlorinated $Ru^{\delta+}$ species [27, 28] given the characteristic bands of $Ru_2(CO)_6Cl$ at 2143 cm^{-1} and 2083 cm^{-1} [28]. The spectrum of the Ru-B catalysts has been reported [12] to have essentially the same peaks as the Ru catalysts and only the peak due to Ru°-CO appears displaced to 2052 cm^{-1} and the peak due to Ru chloride species is shifted to 2133 cm^{-1}. These shifts are attributed to the charge transfer of nonreduced B from Ru, implying strong interactions between them. The Ru-Sn-B catalyst spectra presented in Figure 4 are markedly different (beyond the overall reduction of intensity due to the blocking of Ru sites by Sn) since the peak at 2132 cm^{-1} disappeared completely while the band at 2056 cm^{-1} is increased. Also a new absorption band appears at about 2000 cm^{-1} for the Ru-Sn(0.5) and Ru-Sn(1.0) catalysts which is shifted to 2025 cm^{-1} for the Ru-Sn(2.0) and Ru-Sn(4.0) catalysts. This new band is a sign of the appearance of Ru atoms in a different state and strongly influenced by Sn. The fact that this band appears at a lower wavenumber indicates an electronic transfer from Sn towards Ru. Overall, the changes reflect a strong modification in the electronic density of Ru atoms and presence of small quantities of Ru^{n+} species.

The XPS technique is useful to obtain valuable information about the superficial species in the catalysts. Only the Ru $3d_{5/2}$ peak was used to determine the chemical state of Ru atoms given the superposition between the Ru $3d_{3/2}$ and C 1s peaks. XPS results enabled to determine the binding energies (BE) for Ru° metallic species between 279.2 and 280.1 eV for all catalysts in accordance with previous studies [11, 29, 30].

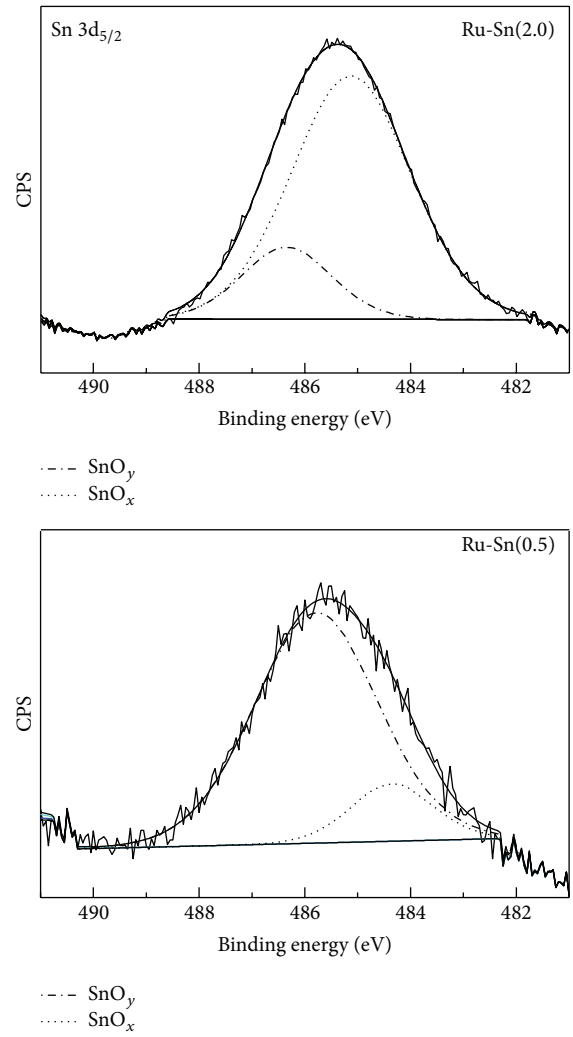

Figure 5: XPS spectra of the bimetallic catalysts in the energy range of the Sn $3d_{5/2}$ core level.

The presence of oxidized Ru species was also confirmed by a Ru $3d_{5/2}$ peak around 284 eV. Incomplete reduction of Ru monometallic catalysts over Al_2O_3 has already been reported [19]. In particular, Elmasides et al. [31] found that approximately 20% of Ru remained in the Ru^{2+} state on Al_2O_3 even after reduction at high temperature (550°C). A single peak found at 192.8 eV (not shown) in the Ru-Sn-B catalyst can be attributed to B^{3+} since B 1s has a peak at 187 eV [32]. From the FTIR-CO results it can be inferred that B is likely adsorbed on the alumina support near the Ru clusters in the form of sodium borate.

The XPS spectra for the bimetallic catalysts are presented in Figure 5 in the BE range of the Sn species (481 to 491 eV). XPS is unable to differentiate Sn^{2+} and Sn^{4+} species given the extremely low BE difference (below 0.5 eV). However, the Sn $3d_{5/2}$ peak which appears at 485 and 486.7 eV can be deconvoluted into two peaks corresponding to SnO_x and SnO_y with $0 < x < y$ as reported by Pouilloux et al. [11]. There are no peaks in the 484-485 eV range, in which Sn°

Table 2: Surface XPS atomic ratios of the metal species on the bimetallic catalysts.

Sn (%)	Ru/Al (bulk)	Ru/Al (XPS)	$Ru^{\circ}/(Ru^{\circ} + Ru^{n+})$	Sn/Al (bulk)	Sn/Al (XPS)	SnO_x (%)	SnO_y (%)
0.5	0.0051	0.0133	0.1439	0.0022	0.0034	14.7	85.3
1.0	0.0052	0.0103	0.2036	0.0044	0.0080	21.4	78.6
2.0	0.0052	0.0101	0.2673	0.0088	0.0196	30.4	69.6
4.0	0.0053	0.0082	0.4634	0.0181	0.0499	24.0	76.0

would be expected, since tin reduction is unable to reach the zero-valent state [15, 18], which is in agreement with the TPR results shown in Figure 1. The majority of the Sn^{4+} is nonetheless reduced to Sn^{2+}, which is strongly stabilized by interaction with the alumina support [33].

XPS data allowed to compute the Ru/Al, Sn/Al, Sn/Ru, and $Ru^{\circ}/(Ru^{\circ} + Ru^{n+})$ surface atomic ratios, as presented in Table 2. In particular, the Ru/Al thus determined is higher than the bulk ratio obtained by chemical analysis. These results show a Ru surface enrichment in all the catalysts; however Ru surface enrichment decreases as Sn content increases. Moreover, the fraction of Ru° increases as the Sn content increases. Pouilloux et al. [11] also found evidence of surface Ru enrichment. The Sn/Al ratio also shows a surface enrichment of Sn which increases with Sn content. It is interesting to analyze the variation of the fraction of SnO_x and SnO_y with Sn content. The results of Table 2 show that the Ru-Sn(2.0) catalysts have the maximum concentration of SnO_x species (30.4%).

Figures 6 and 7 show conversion and selectivity values as a function of time of the bimetallic Ru-Sn-B catalysts. It can be seen that the Ru-Sn(0.5) catalyst with the highest cyclohexane dehydrogenation activity has the lowest activity in hydrogenation of methyl oleate. This unexpected result could be attributed, as proposed by Cheah et al. [10], to the blocking of the metal sites for hydrogen absorption by strongly absorbed carbonyl groups from the esters. This process would lead to an inhibition of the hydrogen adsorption and the following hydrogenation steps. The strong adsorption of the carbonyl group on the Ru-Sn(0.5) has been previously reported (Figure 2). At the end of the catalytic tests the most active catalyst was Ru-Sn(2.0).

In contrast to the results of Pouilloux et al. [11] no heavy esters were detected. Probably their formation was inhibited at the reaction conditions used in this work. *n*-Dodecane was used as a solvent and a high solvent/reactant ratio. In conditions of high dilution the residence time in the adsorbed state should be minimal for reactants, intermediates, and products. Pouilloux et al. [11] have considered that the formation of oleyl oleate occurs over Sn species with no interaction with Ru and that the rate of formation is enhanced by an increase in both Ru and Sn contents. Oleyl oleate was proposed to be an intermediate product. These authors prepared catalysts with 4.1–10 wt% Sn, a much higher content than the one used in this work (0.47–3.5 wt%). This, together with the difference in reaction temperature (Pouilloux et al., 290°C; this work, 270°C) would determine that oleyl oleate is not formed in our case. A lack of this heavy ester in the products mixture has also been reported by Deshpande et al. [34].

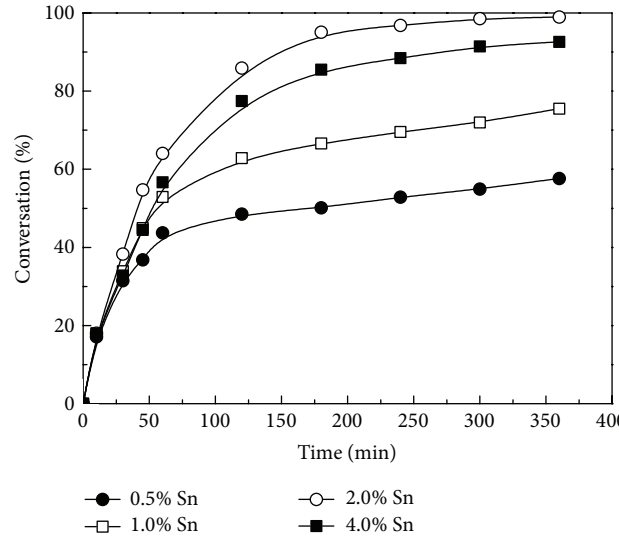

Figure 6: Conversion of methyl oleate as a function of time. Bimetallic catalysts.

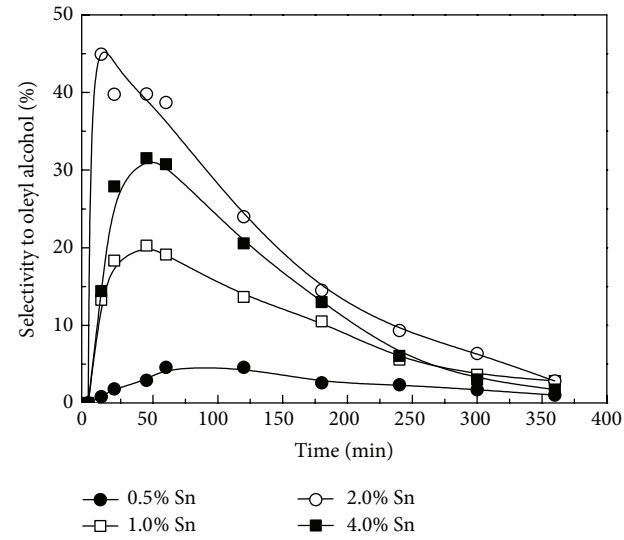

Figure 7: Oleyl alcohol selectivity as a function of reaction time. Bimetallic Ru(1%)-Sn(X%)-B/Al_2O_3 catalysts.

The results for oleyl alcohol selectivity can be seen in Figure 7. A volcano shape indicates that oleyl alcohol is an intermediate product, being formed by hydrogenation of

Table 3: Selectivity to different products at the point of maximum selectivity to oleyl alcohol. Ru(1%)-Sn(X%)-B/Al_2O_3 catalysts.

Sn (%)	Reaction time (min)	Conversion (%)	Selectivity (%)		
			Oleyl alcohol	Stearyl alcohol	Methyl stearate
0.5	60	43.7	4.6	72.1	23.3
1.0	45	45.0	20.3	47.6	32.1
2.0	10	18.0	45.0	10.6	44.4
4.0	60	56.7	32.8	9.3	57.9

oleic methyl ester and being consumed by hydrogenation to stearyl alcohol. The highest selectivity to oleyl alcohol is found for the Ru-Sn(2.0) catalyst in agreement with the findings of Cheah et al. [10] corresponding to a SnO_x/Ru surface ratio of 2, contrary to the report of Pouilloux et al. [11], who have reported a maximum yield for a bulk Sn/Ru atomic ratio of 4.

Table 3 shows the distribution of products in the point of the run of maximum selectivity to oleyl alcohol. Maximum selectivity to oleyl alcohol occurs rather early in the case of the Ru-Sn(2.0) catalyst (10 min and 18% conversion) and much later for the other three catalysts (45–60 min, 43.7–56.7%). Also the maximum selectivity to oleyl alcohol is highest for Ru-Sn(2.0) (45%) and much smaller for the other catalysts (4.6–32.8%). Both effects seem to be related to the relatively high activity for carbonyl hydrogenation and low activity for double bond hydrogenation of the Ru-Sn(2.0) catalyst. Generally speaking, the increase in the Sn content leads to a higher production of methyl stearate indicating that Sn addition decreases the capacity for hydrogenating the CO group while not inhibiting the hydrogenation of the double bond to a great extent. At low Sn content, for example, 0.5%, both the carbonyl and the double bond can be hydrogenated and thus the great production of stearyl alcohol.

Pouilloux et al. [11] reported that the active center for hydrogenating methyl oleate to oleyl alcohol could be a cluster composed of a Ru atom in close interaction with two Sn oxidized species (Ru°-$(SnO_x)_2$). In agreement with this hypothesis the Ru-Sn(2.0) shows the highest amount of SnO_x species and the highest selectivity to oleyl alcohol. Moreover, the results show that tin addition inhibits the CO chemisorption of Ru° atoms and hence also the catalyst capacity for dehydrogenating cyclohexane. At low tin content (0.5 wt%) there is scarce interaction between the Ru and Sn species; tin is in a high oxidation state (SnO_y) and Ru is poorly reduced to the metal state (Table 2). This catalyst could hydrogenate C=C as well as C=O groups forming stearyl alcohol. As the tin content increases, some tin species are drawn closer to the ruthenium particles, either forming mixed species (SnO-Ru) at the alumina-Ru interface or "decorating" ruthenium particles with tin oxides. The interaction between Ru and Sn leads to a higher reduction of Ru thus forming Ru° (Table 2). The concentration of mixed sites (active for the formation of unsaturated alcohols) decreases at higher Sn content (4 wt%) by "decoration" or "encapsulation" of Ru particles by tin oxides.

4. Conclusions

The results of methyl oleate hydrogenation show that Ru(1%)-Sn(2%)-B/Al_2O_3 is the most active and selective material for the production of oleyl alcohol. This was supposed to be due to the relative concentration of Ru and Sn of this sample leading to a better Ru-Sn interaction. At lower Sn concentrations, for example, 0.5%, high amounts of stearyl alcohol are produced since the catalyst presents a higher selectivity towards the hydrogenation of the C=C double bond. Conversely when the Sn content is increased, for example, to 4%, the catalyst shows a low ability for hydrogenating the carbonyl group and can only hydrogenate the double C=C bond, thus unselectively producing methyl stearate.

Conflict of Interests

The authors declare that there is no conflict of interests regarding the publication of this paper.

Acknowledgment

The authors thank Professor Yannick Pouilloux (Institut de Chimie des Milieux et Matériaux de Poitiers, France) for his help with the FTIR-CO characterization experiments.

References

[1] I. V. Deliy, I. L. Simakova, N. Ravasio, and R. Psaro, "Catalytic behaviour of carbon supported platinum group metals in the hydrogenation and isomerization of methyl oleate," *Applied Catalysis A: General*, vol. 357, no. 2, pp. 170–177, 2009.

[2] D. S. Brands, G. U-A-Sai, E. K. Poels, and A. Bliek, "Sulfur deactivation of fatty ester hydrogenolysis catalysts," *Journal of Catalysis*, vol. 186, no. 1, pp. 169–180, 1999.

[3] L. Giraldo, G. Camargo, J. Tirano, and J. C. Moreno-Piraján, "Synthesis of fatty alcohols from oil palm using a catalyst of Ni-Cu supported onto Zeolite," *E-Journal of Chemistry*, vol. 7, no. 4, pp. 1138–1147, 2010.

[4] D. A. Echeverri, J. M. Marín, G. M. Restrepo, and L. A. Rios, "Characterization and carbonylic hydrogenation of methyl oleate over Ru-Sn/Al_2O_3: effects of metal precursor and chlorine removal," *Applied Catalysis A: General*, vol. 366, no. 2, pp. 342–347, 2009.

[5] T. Miyake, T. Makino, S.-I. Taniguchi et al., "Alcohol synthesis by hydrogenation of fatty acid methyl esters on supported Ru-Sn and Rh-Sn catalysts," *Applied Catalysis A: General*, vol. 364, no. 1-2, pp. 108–112, 2009.

[6] M. J. Mendes, O. A. A. Santos, E. Jordão, and A. M. Silva, "Hydrogenation of oleic acid over ruthenium catalysts," *Applied Catalysis A: General*, vol. 217, no. 1-2, pp. 253–262, 2001.

[7] K. De Oliveira, Y. Pouilloux, and J. Barrault, "Selective hydrogenation of methyl oleate into unsaturated alcohols in the presence of cobalt-tin supported over zinc oxide catalysts," *Journal of Catalysis*, vol. 204, no. 1, pp. 230–237, 2001.

[8] K. D. O. Vigier, Y. Pouilloux, and J. Barrault, "High efficiency CoSn/ZnO catalysts for the hydrogenation of methyl oleate," *Catalysis Today*, vol. 195, no. 1, pp. 71–75, 2012.

[9] Y. Pouilloux, F. Autin, A. Piccirilli, C. Guimon, and J. Barrault, "Preparation of oleyl alcohol from the hydrogenation of methyl oleate in the presence of cobalt–tin catalysts," *Applied Catalysis A: General*, vol. 169, no. 1, pp. 65–75, 1998.

[10] K. Y. Cheah, T. S. Tang, F. Mizukami, S.-I. Niwa, M. Toba, and Y. M. Choo, "Selective hydrogenation of oleic acid to 9-octadecen-1-ol: catalyst preparation and optimum reaction conditions," *Journal of the American Oil Chemists' Society*, vol. 69, no. 5, pp. 410–416, 1992.

[11] Y. Pouilloux, F. Autin, C. Guimon, and J. Barrault, "Hydrogenation of fatty esters over ruthenium-tin catalysts; characterization and identification of active centers," *Journal of Catalysis*, vol. 176, no. 1, pp. 215–224, 1998.

[12] M. A. Sánchez, Y. Pouilloux, V. A. Mazzieri, and C. L. Pieck, "Influence of the operating conditions and kinetic analysis of the selective hydrogenation of oleic acid on Ru-Sn-B/Al_2O_3 catalysts," *Applied Catalysis A: General*, vol. 467, no. 10, pp. 552–558, 2013.

[13] M. C. Schoenmaker-Stolk, J. W. Verwijs, and J. J. F. Scholten, "The catalytic hydrogenation of benzene over supported metal catalysts. III. Gas-phase hydrogenation of benzene over silica-supported Ru-Cu catalysts," *Applied Catalysis*, vol. 30, no. 2, pp. 339–352, 1987.

[14] M. A. Sánchez, V. A. Mazzieri, M. Oportus, P. Reyes, and C. L. Pieck, "Influence of Ge content on the activity of Ru-Ge-B/Al_2O_3 catalysts for selective hydrogenation of methyl oleate to oleyl alcohol," *Catalysis Today*, vol. 213, no. 9, pp. 81–86, 2013.

[15] S. A. D'Ippolito, C. R. Vera, F. Epron et al., "Catalytic properties of Pt-Re/Al_2O_3 naphtha-reforming catalysts modified by germanium introduced by redox reaction at different pH Values," *Industrial and Engineering Chemistry Research*, vol. 48, no. 8, pp. 3771–3778, 2009.

[16] M. A. Sánchez, V. A. Mazzieri, M. A. Vicerich, C. R. Vera, and C. L. Pieck, "Influence of the support material on the activity and selectivity of Ru–Sn–B catalysts for the selective hydrogenation of methyl oleate," *Industrial & Engineering Chemistry Research*, vol. 54, no. 27, pp. 6845–6854, 2015.

[17] R. Burch, "Platinum-tin reforming catalysts: I. The oxidation state of tin and the interaction between platinum and tin," *Journal of Catalysis*, vol. 71, no. 2, pp. 348–359, 1981.

[18] B. A. Sexton, A. E. Hughes, and K. Foger, "An X-ray photoelectron spectroscopy and reaction study of Pt-Sn catalysts," *Journal of Catalysis*, vol. 88, no. 2, pp. 466–477, 1984.

[19] V. A. Mazzieri, F. Coloma-Pascual, A. Arcoya, P. C. L'Argentière, and N. S. Fígoli, "XPS, FTIR and TPR characterization of Ru/Al_2O_3 catalysts," *Applied Surface Science*, vol. 210, no. 3-4, pp. 222–230, 2003.

[20] A. Bossi, F. Garbassi, A. Orlandi, G. Petrini, and L. Zanderighi, "Preparation aspects of Ru-supported catalysts and their influence on the final products," *Studies in Surface Science and Catalysis*, vol. 3, pp. 405–416, 1979.

[21] M. Boudart, "Catalysis by supported metals," *Advances in Catalysis*, vol. 20, pp. 153–166, 1969.

[22] C. R. Lederhos, J. M. Badano, N. Carrara et al., "Metal and precursor effect during 1-heptyne selective hydrogenation using an activated carbon as support," *The Scientific World Journal*, vol. 2013, Article ID 528453, 9 pages, 2013.

[23] L. S. Carvalho, C. L. Pieck, M. C. Rangel et al., "Trimetallic naphtha reforming catalysts. I. Properties of the metal function and influence of the order of addition of the metal precursors on Pt–Re–Sn/γ-Al_2O_3–Cl," *Applied Catalysis A: General*, vol. 269, no. 1-2, pp. 91–103, 2004.

[24] J. L. Margitfalvi, I. Borbáth, M. Hegedüs, S. Göbölös, and F. Lónyi, "New approaches to prepare supported Sn–Pt bimetallic catalysts," *Reaction Kinetics and Catalysis Letters*, vol. 68, no. 1, pp. 133–143, 1999.

[25] R. Gomez, V. Bertin, P. Bosch, T. Lopez, P. Del Angel, and I. Schifter, "Pt-Sn/Al_2O_3 sol-gel catalysts: metallic phase characterization," *Catalysis Letters*, vol. 21, no. 3-4, pp. 309–320, 1993.

[26] H. Verbeek and W. M. H. Sachtler, "The study of the alloys of platinum and tin by chemisorption," *Journal of Catalysis*, vol. 42, no. 2, pp. 257–267, 1976.

[27] T. Narita, H. Miura, K. Sugiyama, T. Matsuda, and R. D. Gonzalez, "The effect of reduction temperature on the chemisorptive properties of Ru SiO_2: effect of chlorine," *Journal of Catalysis*, vol. 103, no. 2, pp. 492–495, 1987.

[28] E. A. Seddon and K. R. Seddon, "The chemistry of ruthenium," in *Topics in Inorganic and General Chemistry*, R. J. H. Clark, Ed., chapter 3, Elsevier Science Publisher BV, Amsterdam, The Netherlands, 1984.

[29] S. H. Xie, M. H. Qiao, H. X. Li, W. J. Wang, and J.-F. Deng, "A novel Ru-B/SiO_2 amorphous catalyst used in benzene-selective hydrogenation," *Applied Catalysis A: General*, vol. 176, no. 1, pp. 129–134, 1999.

[30] J. F. Moulder, W. F. Stickle, and P. E. Sobol, *Handbook of X-ray Photoelectron Spectroscopy*, Perkin-Elmer Corporation-Elmer, Waltham, Mass, USA, 1992.

[31] C. Elmasides, D. I. Kondarides, W. Grünert, and X. E. Verykios, "XPS and FTIR study of Ru/Al_2O_3 and Ru/TiO_2 catalysts: reduction characteristics and interaction with a methane-oxygen mixture," *The Journal of Physical Chemistry B*, vol. 103, no. 25, pp. 5227–5239, 1999.

[32] Y. Okamoto, Y. Nitta, T. Imanaka, and S. Teranishi, "Surface characterisation of nickel boride and nickel phosphide catalysts by X-ray photoelectron spectroscopy," *Journal of the Chemical Society, Faraday Transactions 1: Physical Chemistry in Condensed Phases*, vol. 75, pp. 2027–2039, 1979.

[33] S. R. Adkins and B. H. Davis, "The chemical state of tin in platinum-tin-alumina catalysts," *Journal of Catalysis*, vol. 89, no. 2, pp. 371–379, 1984.

[34] V. M. Deshpande, K. Ramnarayan, and C. S. Narasimhan, "Studies on ruthenium-tin boride catalysts II. Hydrogenation of fatty acid esters to fatty alcohols," *Journal of Catalysis*, vol. 121, no. 1, pp. 174–182, 1990.